ORIGINAL ARTICLE

Ultrasound guidance in navigated liver surgery: toward deep-learning enhanced compensation of deformation and organ motion

Jasper N. Smit[1] · Koert F. D. Kuhlmann[1] · Bart R. Thomson[1] · Niels F. M. Kok[1] · Theo J. M. Ruers[1,2] · Matteo Fusaglia[1]

Abstract

Purpose Accuracy of image-guided liver surgery is challenged by deformation of the liver during the procedure. This study aims at improving navigation accuracy by using intraoperative deep learning segmentation and nonrigid registration of hepatic vasculature from ultrasound (US) images to compensate for changes in liver position and deformation.

Methods This was a single-center prospective study of patients with liver metastases from any origin. Electromagnetic tracking was used to follow US and liver movement. A preoperative 3D model of the liver, including liver lesions, and hepatic and portal vasculature, was registered with the intraoperative organ position. Hepatic vasculature was segmented using a reduced 3D U-Net and registered to preoperative imaging after initial alignment followed by nonrigid registration. Accuracy was assessed as Euclidean distance between the tumor center imaged in the intraoperative US and the registered preoperative image.

Results Median target registration error (TRE) after initial alignment was 11.6 mm in 25 procedures and improved to 6.9 mm after nonrigid registration ($p = 0.0076$). The number of TREs above 10 mm halved from 16 to 8 after nonrigid registration. In 9 cases, registration was performed twice after failure of the first attempt. The first registration cycle was completed in median 11 min (8:00–18:45 min) and a second in 5 min (2:30–10:20 min).

Conclusion This novel registration workflow using automatic vascular detection and nonrigid registration allows to accurately localize liver lesions. Further automation in the workflow is required in initial alignment and classification accuracy.

Keywords Image-guided liver surgery · Ultrasound · Electromagnetic tracking · Nonrigid registration

Introduction

During liver surgery, it is of great importance to accurately localize all lesions. Malignant lesions are often clearly visible on diagnostic imaging, but it can be challenging to locate

✉ Jasper N. Smit
j.smit@nki.nl

[1] Department of Surgical Oncology, The Netherlands Cancer Institute–Antoni van Leeuwenhoek, Plesmanlaan 121, 1066CX, Amsterdam, The Netherlands

[2] Nanobiophysics Group (NBP), Faculty of Science and Technology (TNW), University of Twente, Enschede, The Netherlands

all lesions during surgery. Localization is especially difficult when lesions are small, appear isoechoic on intraoperative ultrasound (US), or when they have vanished after neoadjuvant chemotherapy treatment [1, 2]. Surgical navigation may improve localization when preoperative imaging is merged with intraoperative imaging.

Despite several available research systems and continuous improvements in the last decade [3], the use of surgical navigation during liver surgery is still not adopted in clinical practice. Two main challenges can be identified for accurate navigation in liver surgery. First, registration between preoperative imaging and the intraoperative positioning is often performed manually, hindering the workflow as it is time-consuming and prone to errors. Second, the registration is often compromised by an altered organ shape and position of the liver due to laparotomy in open surgery, or CO_2 insufflation in laparoscopic surgery [4, 5]. To tackle these challenges

any movement and deformation of the liver during surgery need to be registered.

To track movement of the liver and to map the amount of deformation, several solutions have been investigated, including optical tracking of liver movement combined with finite element modeling [6–8]. While a subcentimeter surface registration is feasible, finite element modeling requires high computational power which makes real-time intraoperative use difficult. Moreover, instruments or hands in the camera's limited field of view complicate this approach. It has been investigated to improve this technology by using deep learning [9]; its current reliability, however, is still uncertain and compromises intraoperative application at short term. When registration is performed based on the liver surface, it does not guarantee an accurate registration of structures within the parenchyma such as targeted lesions and vasculature.

Instead of optical tracking of the liver contour, liver vasculature can be used for patient-to-image registration with preoperative imaging. Ultrasound imaging of liver vasculature is standard of care during liver surgery and hence easily available. Nevertheless, imaging artifacts regularly occur during image acquisition thereby hindering classical image processing techniques for hepatic vasculature segmentation in US. Recently, deep learning approaches have been evaluated to circumvent these problems [10]. Deep learning-based (DL-based) segmentation enables automated classification between hepatic and portal vasculature which allows for selective registration and improved registration accuracy [11].

Registration accuracy of the segmented vessels to preoperative imaging is influenced by liver movement and deformation. In earlier studies [12, 13], we used electromagnetic (EM) tracking of the liver to compensate for liver movement and rigid registration methods for image registration between intra-operative US imaging and preoperative CT or MR imaging. In the current study, we aim to improve navigation accuracy by compensating for tissue deformation with nonrigid registration. Registration is performed after multi-label deep learning-based segmentation of hepatic vasculature. This method is examined intraoperatively in open liver surgery, after which navigation accuracy is determined at the target lesion.

Materials and methods

A prospective feasibility study was conducted at the Netherlands Cancer Institute, a tertiary referral center for treatment of colorectal liver metastases. The study protocol was approved by the institutional medical ethics committee in July 2018 (NL65724.031.18) and registered in the Netherlands Trial Register (number NL7951). Two phases of the study were designed. In the first phase, the navigation setup as described previously was tested [13]; in the second phase, the deformable (i.e., nonrigid) registration method was evaluated.

Patients were eligible for inclusion when scheduled for open surgery of liver tumors, if the diameter of the target lesion was smaller than 8 cm, if bifurcations of vasculature around the target lesion were present in the preoperative imaging, and if the diagnostic scan was not older than 2 months at the day of surgery. Patients with a pacemaker or large cysts (> 5 cm) in the targeted area were excluded.

Navigation setup and surgical workflow

All details of the navigation setup have been described in a previous study [13]. Electromagnetic tracking (Northern Digital Inc, Waterloo, Ontario, Canada) was used to track an intraoperative US transducer (type I14C5T, BK Medical, Denmark). The tracked transducer allows registration of vasculature as it is visible on intraoperative US and in the patient-specific 3D models which are based on preoperative magnetic resonance imaging (MRI) or computed tomography (CT) scans. Navigation was performed with CustusX navigation software, enabling ultrasound acquisition and visualization of the tracked ultrasound and patient-specific 3D models [14].

For image acquisition, the EM-tracked US transducer was covered by a sterile sleeve, while ensuring that the liver was within the field of view of the EM field generator when US imaging was performed. Next, the surgical workflow of image acquisition starts by attaching an EM sensor close to the targeted lesion with surgical glue (Dermabond® advanced adhesive, Ethicon), followed by an initial registration step and a subsequent ultrasound sweep of the area of interest. After image acquisition a registration workflow is started. An overview of the workflow steps is provided in Fig. 1.

Initial alignment

Nonrigid registration requires an initialization step, consisting of a rough alignment that was performed by initially aligning the coordinate systems of the tracked US with the 3D model, followed by a landmark registration as described by Pérez de Frutos et al. [15]. For this, the imaging plane of the US transducer was aligned to the longitudinal body axis of patient, by pointing the US transducer to the caudal direction of the patient. Afterward, minimally one landmark (mostly a vessel bifurcation) close to the target lesion was digitized. A visual inspection to assure correct initial alignment was performed by assessing the overlay of the registered 3D models on US.
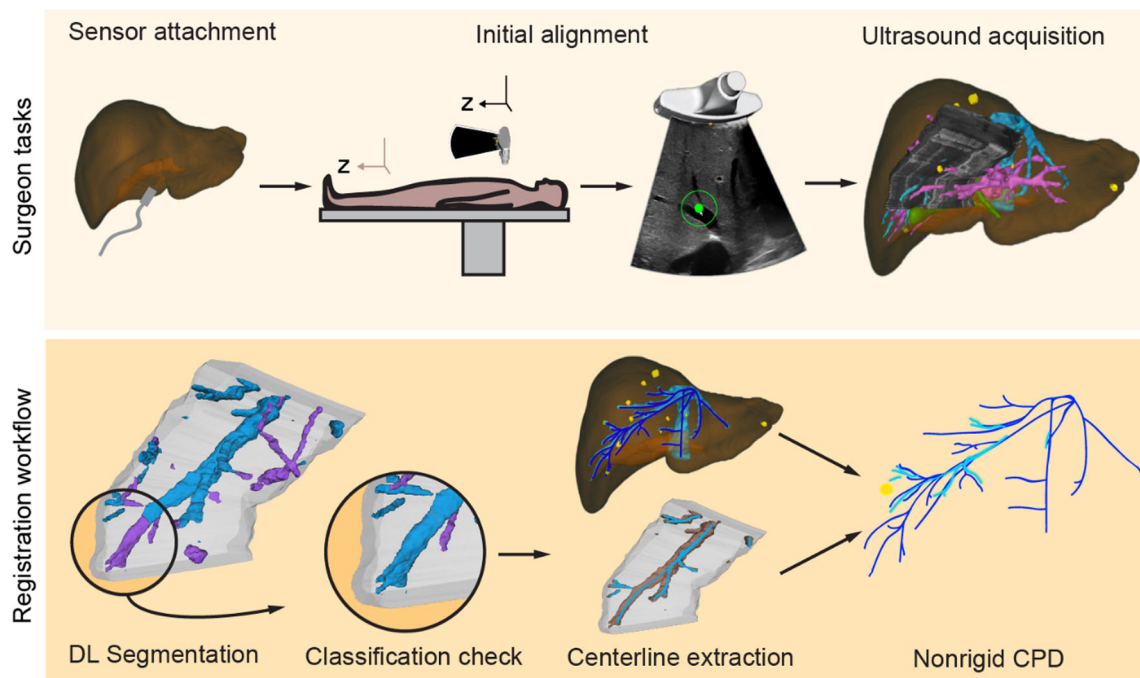
Fig. 1 Workflow overview (DL = deep learning, CPD = coherent point drift)

Ultrasound acquisition

After initial alignment, an ultrasound volume was recorded by sweeping the tracked US transducer over the liver surface. The surgeon was instructed to acquire an US sweep containing at least a main branch of vasculature which enclosed the targeted lesion. The pixels from the single 2D US slices can be placed in a 3D voxel grid, as all 2D slices have specific EM tracking data based on calibration of the transducer. The US volume was reconstructed using Pixel-nearest-neighbor (PNN) reconstruction [16].

Segmentation and nonrigid registration

A 3D U-Net was used for segmentation and classification of portal and hepatic vasculature [11]. This network was based on a conventional 3D U-Net architecture [17], but with a reduced number of filters to minimize memory bottlenecks. Training was performed with the Dice loss function, using 85 US volumes in training and validation.

After inference of the network during surgery, segmentation results were loaded into 3D Slicer together with the US volume for quality control [18]. Wrongly classified vessel branches were corrected if needed. No manual additions were applied to the segmentations. From the segmented vasculature, centerlines were extracted and registered to the corresponding counterparts of vasculature from the preoperative 3D model. A nonrigid coherent point drift algorithm (CPD) was used for registration of the centerlines [19], for which a python implementation was used [20]. Two parameters are tunable in this implementation. First, deformability of the preoperative model was set as $\alpha = 0.3$ (range 0.1–0.5). Second, the width of the smoothing Gaussian kernel was set as $\beta = 550$ (range 50–800). Either the portal vein or the hepatic vein was used for registration, depending on the proximity to the target. Registration of the target lesion was based on the eight closest vectors to the tumor center of mass, extracted from the vector field after the applied nonrigid registration. The specific deformability parameters for CPD and the number of closest vectors were determined by grid search optimization in previous work [11].

If the first registration did not result in a correct overlay on US imaging, a second attempt was performed.

Accuracy and workflow evaluation

Navigation accuracy was evaluated by means of the Target Registration Error (TRE) which was defined as the Euclidean Distance between the center of the tumor in the preoperative scan and the registered intraoperative 3D US. For this purpose, the tumor was delineated in the US volume using the Segment Editor of 3D Slicer. Both the TRE after rough initial alignment and after nonrigid registration were calculated and compared.

For all steps of the navigation process, times were recorded to assess their impact on the surgical workflow. The workflow components were divided into five phases, i.e., sensor

Fig. 2 a Visualization of the 3D scene after initial alignment. **b** The overlay of the registered 3D model on US is not accurately aligned. **c** Vasculature as segmented with DL is visualized in the 3D scene with respect to the tracked transducer. **d** The intraoperative hepatic (blue) and portal (purple) vasculature segmented via DL are accurately projected on US. The location of a poorly visible lesion is indicated (red) adjacent to the actual location of the hypoechoic lesion
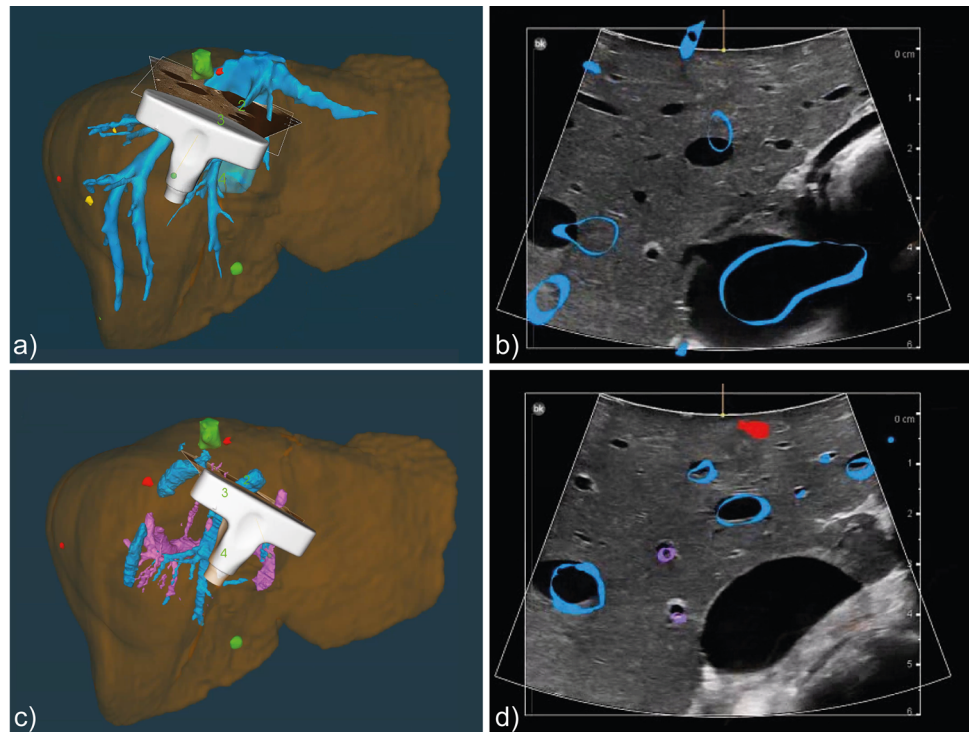
attachment, initial alignment, US acquisition and reconstruction, segmentation and nonrigid registration, and a manual check between segmentation and registration. Additionally, the number of registration attempts per surgery was noted.

Statistical analysis

The study was designed with the aim to achieve a TRE ≤ 10 mm, as this is generally considered as an acceptable threshold in the literature [3]. We aimed to achieve this accuracy in minimally 70% of the navigated procedures. A one-sample Wilcoxon signed-rank test was used to determine whether the median TRE was ≤ 10 mm.

As the automatic registration is dependent on initial alignment, the TRE after automatic registration was considered a paired measurement together with the TRE of initial alignment. Therefore, a pair-wise comparison of manual and automatic registration was performed using the Mann–Whitney U-test to determine whether automatic registration improved accuracy after initial alignment.

Results

Thirty-one patients were included between July 2020 and December 2021. Among these patients, the median diameter of the target lesion was 11 mm (range 4–49). Targeted lesions were located in all segments except segment VII; 20 of 31 targeted lesions (64.5%) were located in the left hemiliver

(segments I-IV). Segment IVa was targeted most often with ten lesions (32.3%).

Registration and navigation were performed in 30 of 31 procedures. In one case, vasculature was not visible near the target lesion which eliminated the possibility of registration and subsequent navigation. In six cases, target registration errors were not calculated. In two of these, hepatic steatosis inhibited sufficient ultrasound quality to carry out DL-based segmentation and therefore registration as well. In one other case, the tumor was not visible in the ultrasound volume. Software problems inhibited display of the tumor location in two cases.

Based on the location of the target lesion, either the portal vein (33.3%) or the hepatic vein (66.7%) was chosen for registration. The middle hepatic vein was most often used (16 out of 30 procedures). The registered vasculature and target lesion, together with the DL segmentation, were loaded in the navigation software to verify their location. An example of initial registration and the intraoperatively segmented vasculature is shown in Fig. 2.
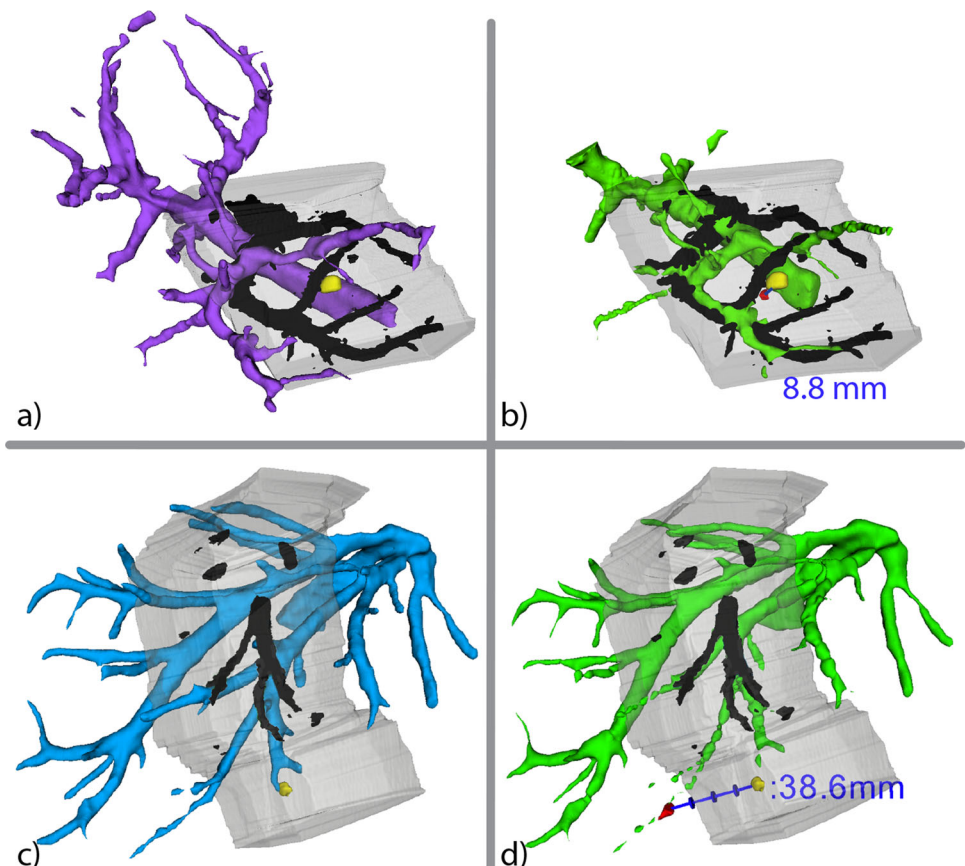
Accuracy evaluation

Intraoperative to preoperative nonrigid vessel registration resulted in a root-mean-squared error of the centerlines of 3.3 ± 1.4 mm. TREs were calculated in 25 navigated procedures. Initial alignment resulted in a median TRE of 11.6 mm (mean 15.4 ± 12.2 mm). Three initial TREs of approximately 35 mm or higher were found after initial alignment
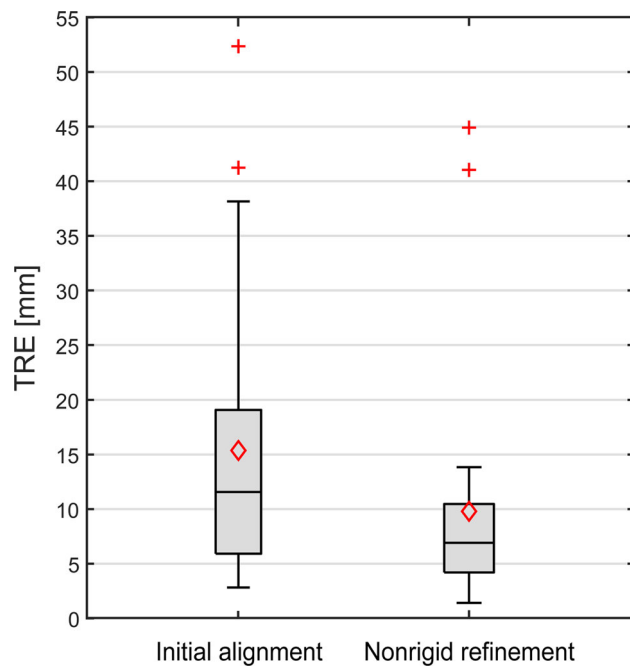
Fig. 3 Comparison of target registration error: manual (rigid) versus automatic (deformable) registration. Median (line) and mean (diamond) are shown
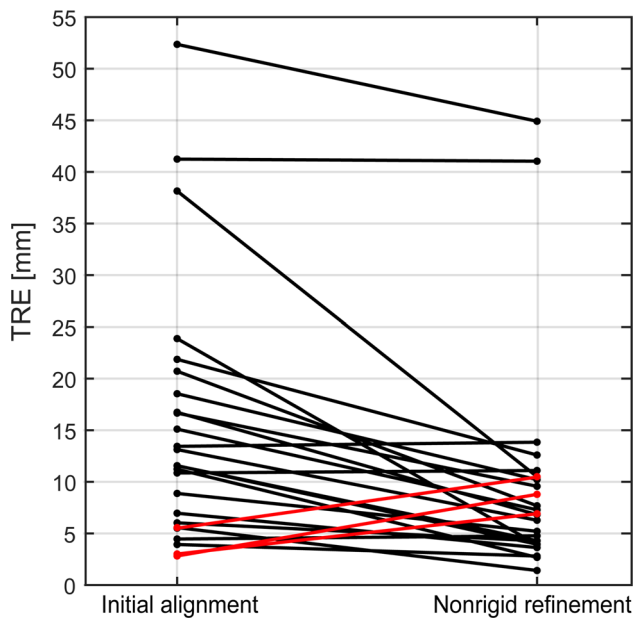
(Fig. 3). All TREs were computed at the center of the target lesion, except in one case where the whole tumor could not be imaged within the US volume. Here, a clear protrusion of the lesion was used. Subsequent refinement by nonrigid registration resulted in a median TRE of 6.9 mm (mean 9.8 $\pm$ 10.3 mm), of which a successful and failed example is shown in Fig. 4.

Accuracy increased significantly from initial alignment to nonrigid refinement ($p = 0.0076$). The Wilcoxon signed-rank test ($\alpha = 0.05$) showed that the median TRE of 6.9 mm was significantly lower than the aimed 10 mm ($p = 0.016$). Additionally, the number of registrations having TREs above 10 mm halved from 16 to 8 after nonrigid registration (Fig. 5). In three cases, the TRE increased, although remained below 10 mm.

Workflow evaluation

The number of attempts for completion of the whole registration workflow (i.e., initial alignment followed by deformable refinement) was one ($n = 21$) or two ($n = 9$). On average, two landmarks were used for initial alignment. The complete workflow was achieved in a median time of 11 min (8:00–18:45 min, detailed breakdown in Table 1). This

Fig. 4 Example of a successful (**a**–**b**) and failed registration (**c**–**d**). **a** An initial alignment of the vasculature in US (black) with the preoperative portal vein (purple) is shown. **b** Nonrigid registration generates a deformed portal vein (green) and positioned the co-registered lesion (red) close to the actual tumor position in US (yellow). **c** The second example shows large angulation after initial alignment of the preoperative (blue) and intraoperative (black) hepatic vein. **d** Nonrigid registration did not result in a correct deformed hepatic vein (green), which resulted in incorrect registration of the tumor

Fig. 5 Pair-wise comparison of initial alignment (left) versus deformable registration (right). Three cases (red) showed a clear increase of TRE after performing deformable registration

Table 1 Required time divided per workflow step

Workflow steps	Median time, min (range)
First registration attempt ($n = 21$)	11:15 (8:00–18:45)
Liver sensor attachment	1:45 (1:00–3:00)
Initial alignment	4:45 (1:45–9:15)
US acquisition and reconstruction	1:15 (0:30–3:00)
DL segmentation and registration	2:25 (0:40–6:30)
Inspection/correction of vein classification	1:45 (0:45–3:20)
Second registration attempt ($n = 9$)	4:45 (2:30–10:20)
Adjustment of initial alignment ($n = 3$)	1:30 (1:00–3:40)
US acquisition and reconstruction ($n = 7$)	0:45 (0:30–1:00)
DL segmentation and registration	2:35 (1:00–3:15)
Inspection/correction of vein classification	1:25 (0:00–4:40)

includes sensor attachment (median: 1:45 min), initial alignment (4:40 min), ultrasound acquisition and reconstruction (1:15 min), inspection and correction of vein classification (1:45 min) and deformable registration (2:25 min). In the cases where a first deformable registration did not provide accurate navigation, a median 4:45 min was needed for a second registration. In these cases, time was mainly spent on acquisition, segmentation and registration of a new US volume, as sensor placement and initial alignment were generally already performed during the first registration attempt.

Discussion

This study demonstrated a new navigation workflow based on deep learning segmentation and classification of hepatic vasculature and subsequent deformable registration. In combination with local EM tracking of the liver, we complement compensation of local liver movement from previous work [13] by integrating nonrigid registration. Results indicate that navigation accuracy was improved by deformable registration when compared to the initial alignment. A rigid initial alignment can often provide sufficient accuracy to enable image guidance. Nevertheless, when organ manipulation occurs and a landmark-based rigid registration does not compensate for the deformation, nonrigid registration becomes essential. This is a step toward a navigation workflow that is less user-dependent than manual registration.

Improvements in initial alignment and automation are still required.

This novel approach has the potential to provide accurate navigation to help the surgical team in finding difficult lesions, such as vanishing or deep-seated lesions, which otherwise would not be found with conventional imaging. Compared to previous studies [21, 22], this approach has the advantage of using 3D information which compensates for deformation between the preoperative scan and intraoperative liver positioning.

Only in patients with liver steatosis segmentation of vasculature was poor. This may be explained by underrepresentation of steatosis in training data. If segmentation results would improve here, surgical navigation could contribute during these procedures in which retrieval of lesion locations is even more difficult than in homogeneous parenchyma.

Initial alignments of up to 25 mm are positively corrected with the nonrigid registration. Especially in the presence of subcentimeter lesions, this approach shows potential benefit when rigid alignment does not reveal the locations of these small lesions. The hypothesis that nonrigid registration would increase navigation accuracy is confirmed by the observed TREs. The decreased number of procedures with errors above 10 mm supports this claim. Nevertheless, it was observed that when wrong landmarks were selected and thus initial alignment failed, the nonrigid CPD algorithm could not compensate. The two outliers where deformable registration did not result in correct tumor locations, encountered a large offset in both orientation and translation during initial alignment of the middle hepatic vein. As different bifurcations of the hepatic vein often have a similar shape, a correct rough alignment is key to initialize a correct deformable alignment.

In the majority of previous studies, automatic registration requires manual initial alignment. Our two-step registration

approach is comparable to previous studies [23, 24]. Contrary to these studies, we use a deformable registration method instead of a conventional Iterative Closest Point algorithm. Similar to Clements et al. [25] a deformable registration was implemented; however, we apply it on intraparenchymal structures rather than the liver surface. In contrast to these studies, two advantages of our methodology are validation on a larger patient group and accuracy evaluation at the center of the tumor, as it is the most clinically relevant structure.

The computational part of the navigation workflow, i.e., the segmentation and deformable registration, can be performed in approximately one minute which is concordant with a previous study [11]. However, with all steps prior to registration, the total time rapidly increases to 8 min (see Table I). The amount of time required for a manual initial alignment and the manual check and classification corrections caused the largest additional time increase to the workflow. Another time-consuming factor was caused by switching between the navigation software (CustusX), the segmentation framework (a python-based pipeline) and 3D Slicer for quality checks of segmentation. Software switching and data transfer between the different software platforms caused considerable delay, as well as many interactions by the technical physician who assisted the surgeons in the navigation process. Currently, such additional personnel is still needed to perform the current navigation protocol. In future, we aim for an improved integration of all workflow components within one application requiring less user-interactions.

The fact that the second attempts after failure of the first registration cycle were always of shorter duration is mostly caused by the already performed sensor placement and initial alignment. In most of these cases, the second registration cycle started at a new acquisition because the acquisition from the first registration cycle did not provide a good registration. This was mostly caused by an insufficient amount of vasculature in the US volume, or by a low-quality ultrasound acquisition.

Strengths of this study include the combined use of 3D US segmentation and classification of vasculature, deformation compensation, and active tracking of the liver. Progress is made toward an approach where the surgeon is provided with guidance during resection, where the EM sensor is placed near the target lesion as close as possible. While Pelanis et al. [26] propose to update a registration using fluoroscopy based on injected radiopaque fiducials, an EM-based method for local liver tracking provides an improved and more robust way of tracking organ movement. Our approach prevents additional radiation and interruption of the surgical workflow and provides a more continuous stream of tumor tracking eliminating the need for single snapshots in time as needed by fluoroscopy.

Limitations of this study include the non-even spread of tumor targets throughout the liver. Registration was mainly limited to the middle hepatic vein. For lesions surrounding the right hepatic vein in the dorsal segments VI and VII, investigation of the method was limited. These lesions are more difficult to approach and sensor placement near the target lesions is only possible after full mobilization of the liver, inducing considerable deformation. It would also be interesting to further investigate the portal vein for registration as it was underrepresented in the current study.

The manual check of the DL-based vessel segmentation and classification currently delays the surgical workflow. Preferably this step is omitted. At this stage of development, the manual checks were still required to prevent the registration of wrongly classified vasculature, which would require another registration attempt. Right now, classification was performed by the 3D U-net. An alternative is to perform segmentation of all vasculature followed by classification by a connected components algorithm or another DL network.

As possible addition to the proposed registration framework, improvements are required in the process of the initial alignment. Searching for a correct bifurcation fiducial can be time-consuming, and adding fiducials to improve the initial registration is undesirable. This could be solved by using content-based image registration as performed by Ramalhinho et al. [27]. As their solution was initially developed for laparoscopic US to CT registration where less deformation is expected, this approach asks for additional validation in the open setting. Their results indicate that an initial alignment of 20 mm or less is feasible, which could be followed by the proposed deformable registration in this study.

While the nonrigid registration compensates for deformation between the preoperative scan and the intraoperative situation, it does not compensate for differences in ultrasound transducer pressure or, more importantly, movements after surgical manipulation. Further focus should therefore be devoted to maintaining the accuracy after registration, i.e., during the process of resection or ablation. Maintaining navigation accuracy is partially aimed for in the described set-up by using local liver tracking with an EM sensor, but this approach is not all-encompassing. A possible solution is to update the registration with content-based image retrieval for which a 2D US vessel segmentation network is required [22]. As their approach aims to register intraoperative US to preoperative CT, US to US registration could be more accurate for registration updates as this provides more common features. Application is potentially useful during ablation, in which US is continuously used for needle placement and confirmation of a correct ablation zone [28].

Conclusion

The combination of DL-based segmentation of hepatic vasculature and deformable registration improves navigation accuracy during open liver surgery. In cases where lesions are small and deformation is large, this approach is beneficial when compared to rigid registration. Improvements are needed in the initial alignment and automation of the workflow.

Declarations

Conflict of interest Theo Ruers is Chief Medical Officer of Bcon Medical. All other authors have no relevant financial or non-financial interests to disclose.

Ethical approval The study was performed in accordance with the ethical standards of the institutional medical ethics committee and with the 1964 Helsinki Declaration and its later amendments or comparable ethical standards.

Informed consent Informed consent was obtained from all individual patients included in the study.

References

1. Ellebæk SB, Fristrup CW, Mortensen MB (2017) Intraoperative ultrasound as a screening modality for the detection of liver metastases during resection of primary colorectal cancer-a systematic review. Ultrasound Int Open 3:E60–E68. https://doi.org/10.1055/s-0043-100503
2. Kuhlmann K, van Hilst J, Fisher S, Poston G (2016) Management of disappearing colorectal liver metastases. Eur J Surg Oncol 42:1798–1805. https://doi.org/10.1016/J.EJSO.2016.05.005
3. Schneider C, Allam M, Stoyanov D, Hawkes DJ, Gurusamy K, Davidson BR (2021) Performance of image guided navigation in laparoscopic liver surgery–a systematic review. Surg Oncol 38:101637. https://doi.org/10.1016/j.suronc.2021.101637
4. Heizmann O, Zidowitz S, Bourquain H, Potthast S, Peitgen HO, Oertli D, Kettelhack C (2010) Assessment of intraoperative liver deformation during hepatic resection: prospective clinical study. World J Surg 34:1887–1893. https://doi.org/10.1007/S00268-010-0561-X/TABLES/2
5. Vijayan S, Reinertsen I, Hofstad EF, Rethy A, Hernes TAN, Langø T (2014) Liver deformation in an animal model due to pneumoperitoneum assessed by a vessel-based deformable registration. Minim Invasive Ther Allied Technol 23(5):279–286. https://doi.org/10.3109/13645706.2014.914955
6. Golse N, Petit A, Lewin M, Vibert E, Cotin S (2020) Augmented reality during open liver surgery using a markerless non-rigid registration system. J Gastrointest Surg 25:662–671. https://doi.org/10.1007/S11605-020-04519-4
7. Haouchine N, Cotin S, Peterlik I, Dequidt J, Lopez MS, Kerrien E, Berger MO (2015) Impact of soft tissue heterogeneity on augmented reality for liver surgery. IEEE Trans Vis Comput Graph. https://doi.org/10.1109/TVCG.2014.2377772
8. Heiselman JS, Clements LW, Collins JA, Weis JA, Simpson AL, Geevarghese SK (2017) Characterization and correction of intraoperative soft tissue deformation in image-guided laparoscopic liver surgery. J Med Imag 5:1. https://doi.org/10.1117/1.jmi.5.2.021203
9. Pfeiffer M, Riediger C, Weitz J, Speidel S (2019) Learning soft tissue behavior of organs for surgical navigation with convolutional neural networks. Int J Comput Assist Radiol Surg. https://doi.org/10.1007/s11548-019-01965-7
10. Ciecholewski M, Kassjański M (2021) Computational methods for liver vessel segmentation in medical imaging: a review. Sensors 21:2027. https://doi.org/10.3390/s21062027
11. Thomson BR, Smit JN, Ivashchenko OV, Kok NFM, Kuhlmann KFD, Ruers TJM, Fusaglia M (2020) MR-to-US registration using multiclass segmentation of hepatic vasculature with a reduced 3D U-net. In: LNCS, Medical image computing and computer assisted intervention–MICCAI. 12263: 275–284. https://doi.org/10.1007/978-3-030-59716-0_27
12. Ivashchenko OV, Kuhlmann KFD, Veen R, Pouw B, Kok NFM, Hoetjes NJ, Smit JN, Klompenhouwer EG, Nijkamp J, Ruers TJM (2021) CBCT-based navigation system for open liver surgery: accurate guidance toward mobile and deformable targets with a semi-rigid organ approximation and electromagnetic tracking of the liver. Med phys 48(5):2145–2159
13. Smit JN, Kuhlmann KFD, Ivashchenko OV, Thomson BR, Langø T, Kok NFM, Fusaglia M, Ruers TJM (2022) Ultrasound-based navigation for open liver surgery using active liver tracking. Int J Comput Assist Radiol Surg 17(1765):1773. https://doi.org/10.1007/s11548-022-02659-3
14. Askeland C, Solberg OV, Bakeng JBL, Reinertsen I, Tangen GA, Hofstad EF, Iversen DH, Våpenstad C, Selbekk T, Langø T, Hernes TAN, Olav Leira H, Unsgård G, Lindseth F (2016) CustusX: an open-source research platform for image-guided therapy. Int J Comput Assist Radiol Surg 11:505–519. https://doi.org/10.1007/s11548-015-1292-0
15. Pérez de Frutos J, Hofstad EF, Solberg OV, Tangen GA, Lindseth F, Langø T, Elle OJ, Mårvik R (2018) Laboratory test of single landmark registration method for ultrasound-based navigation in laparoscopy using an open-source platform. Int J Comput Assist Radiol Surg 13:1927–1936. https://doi.org/10.1007/s11548-018-1830-7
16. Gobbi DG, Peters TM (2002) Interactive intra-operative 3D ultrasound reconstruction and visualization. Med Image Comput Comput Assist Interv 2489:156–163. https://doi.org/10.1007/3-540-45787-9_20
17. Çiçek Ö, Abdulkadir A, Lienkamp SS, Brox T, Ronneberger O (2016) 3D U-Net: learning dense volumetric segmentation from sparse annotation. In: lecture notes in computer science (including subseries lecture notes in artificial intelligence and lecture notes in bioinformatics). 9901: 424–432. https://doi.org/10.1007/978-3-319-46723-8_49
18. Fedorov A, Beichel R, Kalpathy-Cramer J, Finet J, Fillion-Robin JC, Pujol S, Bauer C, Jennings D, Fennessy F, Sonka M, Buatti J, Aylward S, Miller JV, Pieper S, Kikinis R (2012) 3D slicer as an image computing platform for the quantitative imaging network. Magn Reson Imag. https://doi.org/10.1016/j.mri.2012.05.001
19. Myronenko A, Song X (2010) Point set registration: coherent point drifts. IEEE Trans Pattern Anal Mach Intell 32:2262–2275. https://doi.org/10.1109/TPAMI.2010.46
20. Khallaghi S (2017) Pure numpy implementation of the coherent point drift algorithm. http://siavashk.github.io/2017/05/14/coherent-point-drift. Accessed 12 Jul 2020
21. Mishra D, Chaudhury S, Sarkar M, Manohar S, Soin AS (2018) Segmentation of vascular regions in ultrasound images: a deep learning approach. Proceedings—IEEE international symposium on circuits and systems 2018. https://doi.org/10.1109/ISCAS.2018.8351049

22. Montaña-Brown N, Ramalhinho J, Allam M, Davidson B, Hu Y, Clarkson MJ (2021) Vessel segmentation for automatic registration of untracked laparoscopic ultrasound to CT of the liver. Int J Comput Assist Radiol Surg. https://doi.org/10.1007/s11548-021-02400-6

23. Banz VM, Müller PC, Tinguely P, Inderbitzin D, Ribes D, Peterhans M, Candinas D, Weber S (2016) Intraoperative image-guided navigation system: development and applicability in 65 patients undergoing liver surgery. Langenbecks Arch Surg 401:495–502. https://doi.org/10.1007/s00423-016-1417-0

24. Ribes D, Peterhans M, Anderegg S, Banz V, Candinas D, Weber S (2012) Towards higher precision in instrument guided liver surgery: automatic alignment of 3D ultrasound with pre-operative mevis-ct. Int J Comput Assist Radiol Surg 7(Suppl 1):141–145. https://doi.org/10.1007/s11548-012-0713-6

25. Clements LW, Collins JA, Weis JA, Simpson AL, Kingham TP, Jarnagin WR, Miga MI (2017) Deformation correction for image guided liver surgery: an intraoperative fidelity assessment. Surgery 162:537–547. https://doi.org/10.1016/J.SURG.2017.04.020

26. Pelanis E, Teatini A, Eigl B, Regensburger A, Alzaga A, Kumar RP, Rudolph T, Aghayan DL, Riediger C, Kvarnström N, Elle OJ, Edwin B (2021) Evaluation of a novel navigation platform for laparoscopic liver surgery with organ deformation compensation using injected fiducials. Med Image Anal. https://doi.org/10.1016/j.media.2020.101946

27. Ramalhinho J, Tregidgo HFJ, Gurusamy K, Hawkes DJ, Davidson B, Clarkson MJ (2021) Registration of untracked 2D laparoscopic ultrasound to ct images of the liver using multi-labelled content-based image retrieval. IEEE Trans Med Imag 40:1042–1054. https://doi.org/10.1109/TMI.2020.3045348

28. Van Cutsem E, Cervantes A, Adam R et al (2016) ESMO consensus guidelines for the management of patients with metastatic colorectal cancer. Ann Oncol 27:1386–1422. https://doi.org/10.1093/ANNONC/MDW235